Computers and Electrical Engineering 89 (2021) 106910

Contents lists available at ScienceDirect

Computers and Electrical Engineering

journal homepage: www.elsevier.com/locate/compeleceng

Simulation and experimental design of adaptive-based maximum power point tracking methods for photovoltaic systems

P. Srinivasarao [a], K. Peddakapu [b], M.R. Mohamed [b,*], K.K. Deepika [c], K. Sudhakar [d,e]

[a] Department of Electrical & Electronic Eng., Nalanda Institute of Eng. &Tech., A.P, India
[b] College of Engineering., Universiti Malaysia Pahang, Kuantan, Malaysia
[c] Department of Electrical & Electronic Eng., Vignan's Institute of Information Technology, India
[d] Faculty of Mechanical and Automotive Engineering Technology., Universiti Malaysia Pahang, Pekan, Malaysia
[e] Automotive Engineering Centre, Universiti Malaysia Pahang, Pekan 26600, Pahang, Malaysia

ARTICLE INFO

Keywords:
PV system
MPPT
Temperature
Irradiation
Adaptive FPIDN
Boost converter

ABSTRACT

This paper presents a filter-based adaptive fuzzy proportional integral derivative (FPIDN) controller for photovoltaic (PV) systems. The proposed maximum power point tracking (MPPT) method is implemented in two blocks. The first block represents by an adaptive calculation block; to produce a reference voltage for every maximum power point (MPP), whereas the second is the FPIDN controller; utilized to manage duty cycle of the PWM converter. The effectiveness of the proposed MPPT has been evaluated to different MPPT methods. The efficiency of the proposed MPPT recorded at 99.45% and 99.72% with MPP capture time clocks at 0.048s, outperforms the benchmarked traditional MPPT methods under diverse irradiance and temperature conditions.

1. Introduction

Nowadays, several countries are adopting enthusiastic policies on the deployment of renewable energy technologies in order to mitigate the detrimental effects on the environment. The rapid development of renewable sources has been observed in several countries over the last decade. Solar energy is a very attractive and abundant form of energy among the other renewable energy sources. In addition, it is easy to buy, requires needs less maintenance, and inexhaustible. However, the challenge of the PV system is to transform solar energy into electrical energy due to continuous changes in atmospheric conditions such as irradiance and temperature [1].

In recent years, numerous research studies have focused on the different types of MPPT methods to extract the maximum power from the PV panels. The objective of these MPPT methods is to transmit the maximum power from the PV system to the load or grid demand by managing the converter duty cycle under different weather conditions. Many of the MPPT methods are presented in the literature [2,3] for acquiring the maximum power. Furthermore, the perturbation and observation (P&O) is one of the notable MPPT methods to obtain maximum power. It is simple to implement, low cost, and display good performance [4].

In the case of the P&O process, when the maximum power point (MPP) is reached, the operating point fluctuates as a result of the oscillating feature. Moreover, when the atmospheric conditions change suddenly, it would be difficult to assess the variation in power

This paper is for regular issues of CAEE. Reviews processed and recommended for publication to the Editor-in-Chief by Associate Editor Dr. G. Glan Devadhas.

* Corresponding author.
E-mail address: rusllim@ump.edu.my (M.R. Mohamed).

https://doi.org/10.1016/j.compeleceng.2020.106910
Received 2 January 2020; Received in revised form 5 November 2020; Accepted 12 November 2020

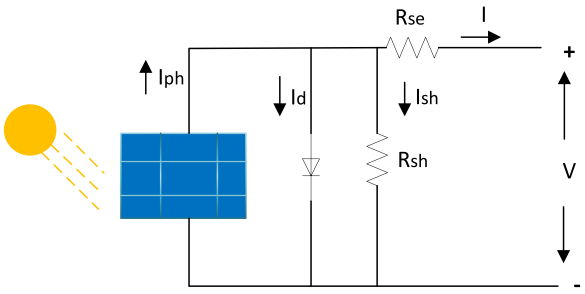

Fig. 1. Representation of the solar cell with a single diode.

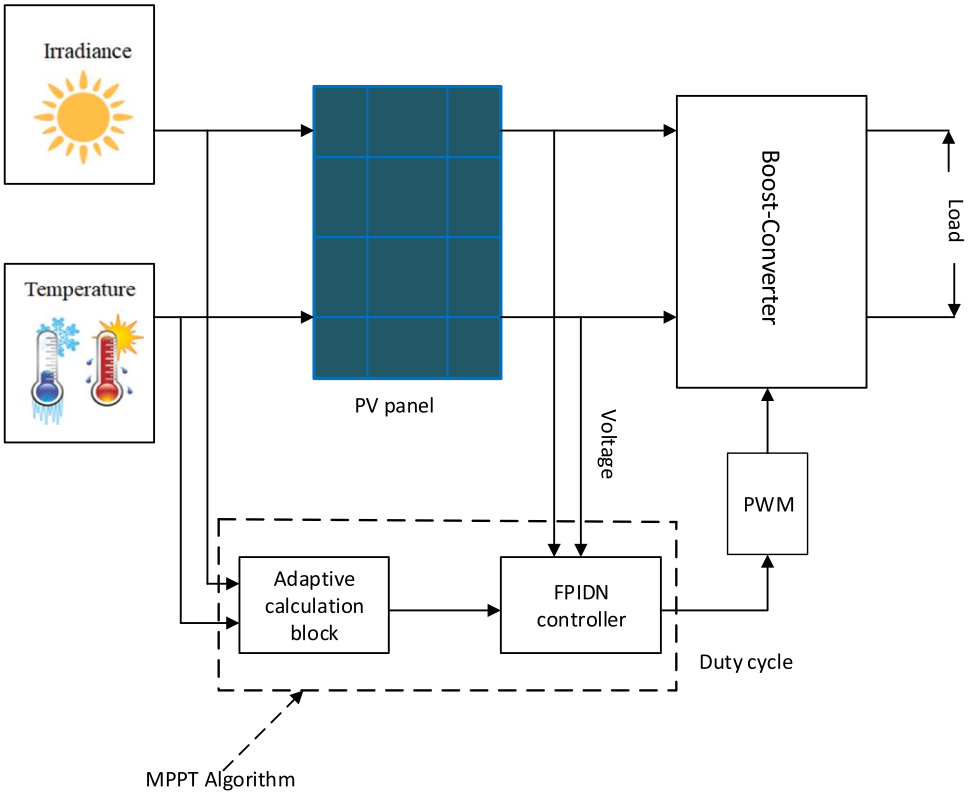

Fig. 2. Block diagram of the PV system with the FPIDN controller.

is caused by environmental situations or usage of perturbation size. The overall performance of the PV system can therefore be reduced by these difficulties.

Another unique method is incremental conductance (Inc.Cond.), which provides the most satisfactory results in terms of speed, accuracy, and efficiency than the P&O method. This algorithm is more suitable for the PV system to monitor the maximum power at sudden changes in solar irradiance [5]. The layout of this methods is complex, and the accuracy of the method depends on the size of the iteration. A fast-converging MPPT method is proposed in the PV system to increase the boost converter voltage [6,7]. In addition, this method decreases the complexity of the structure and shows high performance over conventional incremental conductance (Inc. Cond). Some researchers [8–10] have presented the modified Inc.Cond. method in the PV system to improve the tracking capability under fast-changing solar irradiance. However, the modified Inc.Cond. and P&O may not produce the correctness and speed in attaining the MPP during a large variation of solar irradiance.

Conventional controller-based MPPT methods such as proportional-integral (PI), proportional integral derivative (PID), integral double derivative (IDD) controllers are implemented in the PV system to manage the duty cycle of the PWM-based converter [11–13]. Since traditional controllers are used in the PV system, the system response time, overshoot, and undershoot is high, which can lead to system failure in partial shading situations. Recently, many experiments [14–16] have been performed on artificial intelligence (AI) methods to address the drawbacks of conventional methods. Gowid and Massoud [17] proposed an artificial neural network (ANN)-based MPPT methods for the attainment of maximum power from the PV panel using the backpropagation algorithm. But it

takes a tremendous amount of time to train the data and operate properly. Another AI technique is a fuzzy logic controller (FLC) [18], used in the PV system to control the voltage of the boost converter. Rezk et al. [19] have developed an adaptive fuzzy logic-based novel MPPT method for estimating the converter duty cycle. It shows the prolific performance in attaining MPP at stable and variable conditions compared to conventional Inc.Cond. and P&O. These intelligent methods have led to the productive outcomes in terms of performance, accuracy, and robustness under partial shading circumstances. While AI and traditional MPPT-based controller methods are evaluated separately in the PV system, the joint operation of both controllers has not yet been studied with the PV system. Hence, it is therefore essential to evaluate with the PV system in order to improve the tracking ability.

In this work, a fuzzy assisted integer order proportional integral derivative with filter (FPIDN)-based MPPT method is suggested in the PV system to improve the tracking capability under different weather conditions. The inputs of the PV system are temperature and irradiance, assigned to the input parameters of the FLC. Since the reference voltage for MPP is measured in the adaptive calculation module, the usage of membership functions in the fuzzy method is lessened. As a result, the MPPT tracking ability has been enhanced and the variations around MPP have decreased. In addition, the output of the FLC shall serve as the input of the PIDN controller. The output signal is produced from the PIDN to adjust the booster converter switch to maintain a better voltage profile. Both simulation and experimental results show that the proposed adaptive FPIDN-based MPPT controller provides better performance in terms of precision, speed, and efficiency.

The paper is organized as follows: the modelling of the PV system is illustrated in section 2. The structure of the adaptive FPIDN based MPPT method is discussed in Section 3. The simulation results and discussions are presented in Section 4. Experimental validations are shown in Section 5. Eventually, the concluding remarks are provided in Section 6.

2. Mathematical modelling of the PV system

The most prevalent model utilized to demonstrate the PV cell is a single diode model. In this model, shunt and series resistances (R_{sh} & R_{se}) are connected to a diode with a current source and shown in Fig. 1 [18,19]. The block diagram of the suggested PV system with the FPIDN controller is demonstrated in Fig. 2.

As per Kirchhoff's law, the resultant current equation of the PV cell is denoted as [18]:

$$I = I_{ph} - I_d - I_{sh} \tag{1}$$

Where I is the resultant current, I_{ph} indicates the PV current without power loss and it varies with the atmospheric conditions. Also, the leakage current in shunt resistance is identified with I_{sh} and the current flow in the diode is I_d.

$$I_d = I_O\left(e^{q\frac{(V+IR_s)}{n.KT}-1}\right) \tag{2}$$

Where I_O is represented as reverse saturation current of diode, q is a charge of the electron (1.60217 × 10^-19 C), n is diode factor, K is Boltzmann constant (1.3806 × 10^-23 J/K) [18,19], and T is the p-n junction temperature in Kelvin (K).

The PV current (I_{ph}) depends on the weather conditions and is cited in (3) [18,19].

$$I_{ph} = \frac{G}{G_{STC}}\left(\left(I_{sc,STC} + C_I(T - T_{STC})\right)\right) \tag{3}$$

Where $I_{sc,STC}$ is the short-circuit current (SC) at standard test condition (STC), C_I is the temperature coefficient of SC, T_{STC} is the temperature value at STC, and G_{STC} is considered as the irradiation value of the solar panel at STC.

Eq. (1) can be written as [18]:

$$I = I_{ph} - I_O\left(e^{q\frac{(V+IR_s)}{n.KT}-1}\right) - \frac{V + R_{se}I}{R_{sh}} \tag{4}$$

Where I_O demonstrates the diode reverse saturation current and expressed as [18]:

$$I_0 = I_{0,STC}\left(\frac{T}{T_{STC}}\right)^3 \exp\left(\frac{qE_G}{n.K}\right)\left(\frac{1}{T} - \frac{1}{T_{STC}}\right) \tag{5}$$

E_G is donated as the semiconductor band energy in eV, (for Si 1.12 eV).

The standard saturation current is $I_{0,STC}$, which can be calculated as [18,19]:

$$I_{0,STC} = \frac{I_{sc,STC}}{\exp\left(\frac{V_{oc,STC}}{b.V_{t,STC}} - 1\right)} \tag{6}$$

Where $V_{t,STC}$ is the PV panel terminal voltage at standard temperature, and b is the diode constant (typically,$1 \le b \le 1.5$). The maximum power generated through a single PV cell is very less (1-1.52 W).

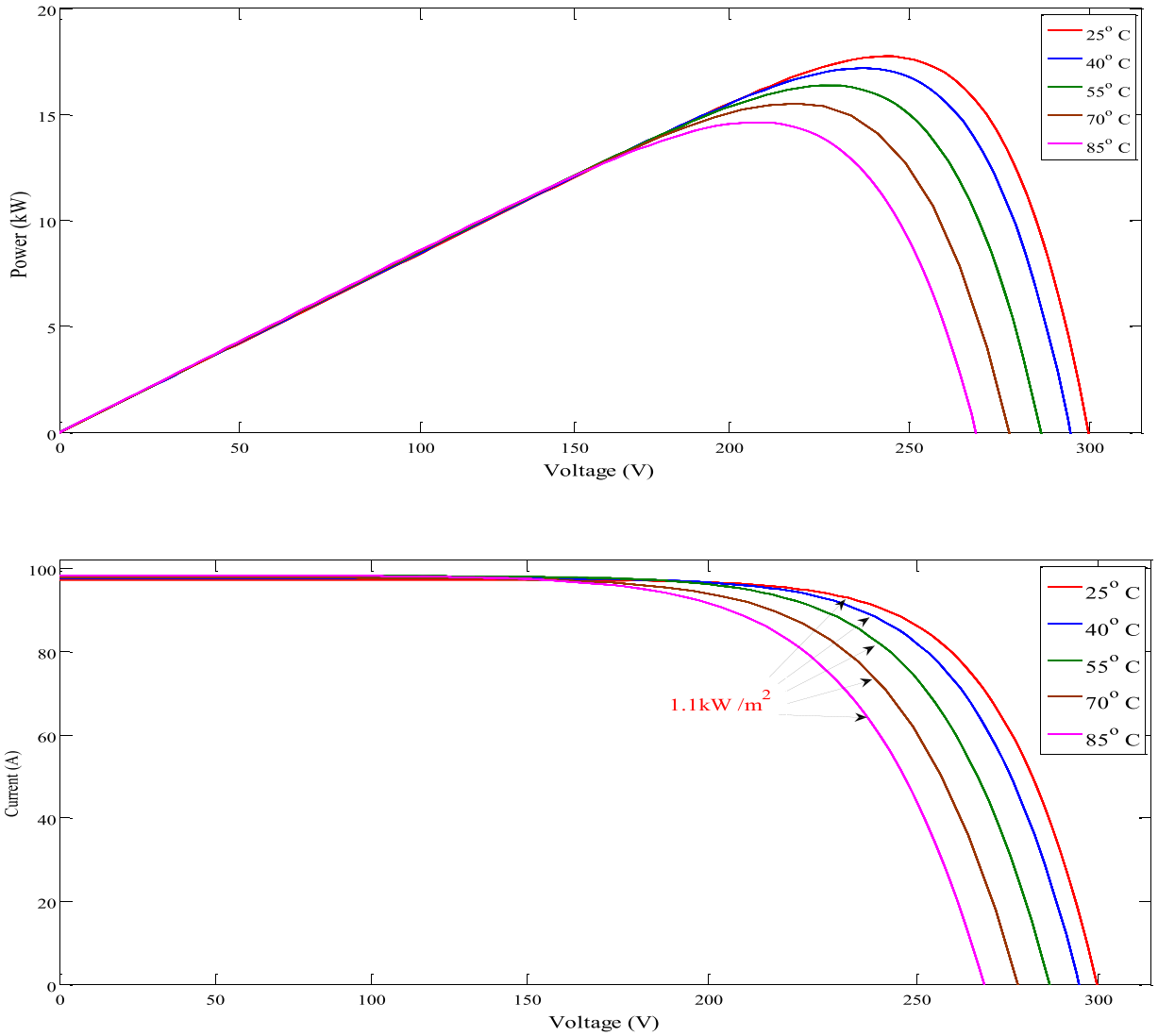

(a) P-V and I-V (at various temperatures °C)

Fig. 3. Characteristics of the PV at various atmospheric conditions.

The solar PV cells should be connected in series in order to acquire the necessary amount of power from the PV array. The electrical characteristics like P-V and I-V of PV arrays under varying temperatures and irradiance levels are illustrated in Fig. 3. The PV panel electrical parameters are reported in Table 1.

3. Design of adaptive FPIDN-based MPPT method

Traditional PID controllers have mostly been used in the PV system in recent decades to design effective MPPT algorithms and to improve the tracking capabilities under rapid changes in solar irradiance and temperatures [20]. The various provisions of the PID controller are simple structure, compact design, lower cost, and generates productive results for linear systems. However, when the system becomes extensive with diverse sources, traditional controllers may not produce reliable outcomes. In addition, PID controllers are not ideal for time-delay systems and high order systems with uncertainties.

Conversely, the fuzzy logic controller (FLC) is one of the powerful methods among AI methods to resolve the drawbacks of the conventional controllers [18]. It represents human decision- making and is entirely based on fuzzy logic theory. The most important feature of the FLC is to upgrade the input and output parameters for each control cycle. However, the FLC most challenging task is to align the rule base and membership functions (MF) in a constructive manner. It takes a long time, making the machine speed slow and

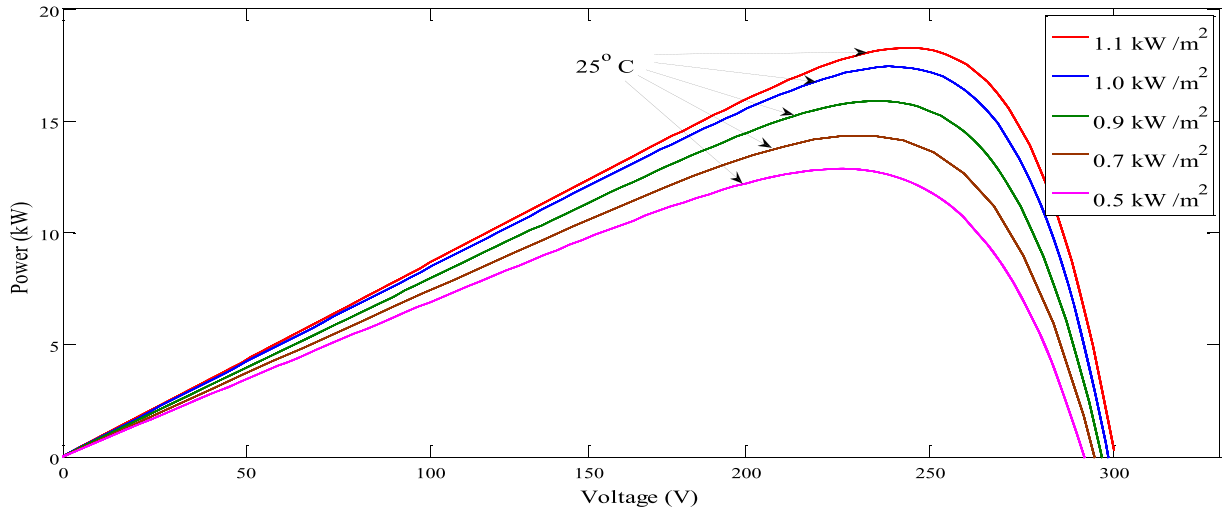

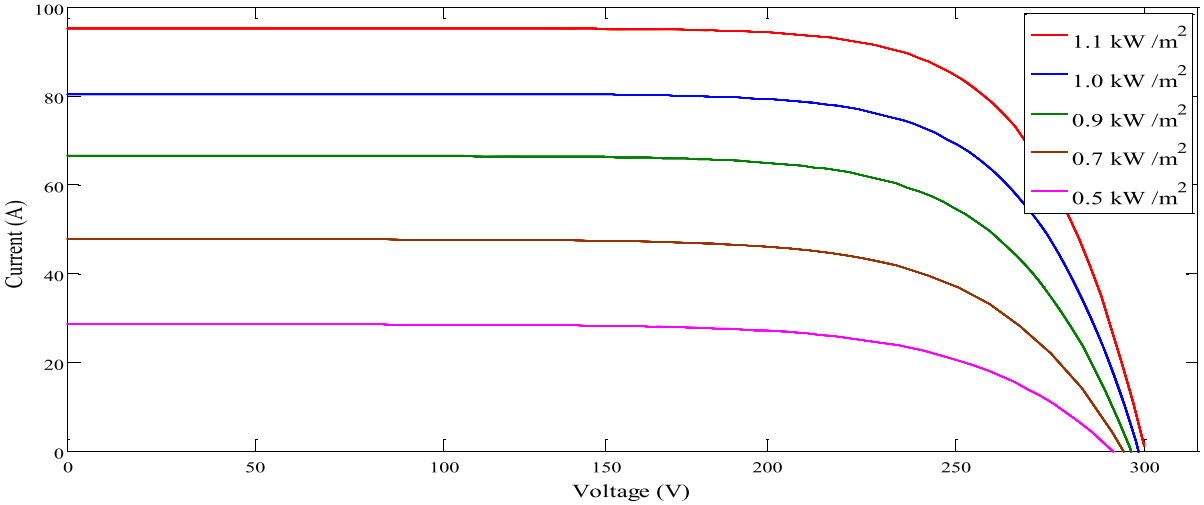

(b) P-V and I-V (at various irradiance levels in W/m2)

Fig. 3. (*continued*).

Table 1
PV panel electrical parameters.

Parameters	Value
I_{sc}	8.15 A
V_{oc}	29.87 V
I_{mpp}	7.52 A
V_{mpp}	24.48
K_I	0.029 A/K
K_V	−0.33 V/K
N_S	48

difficult to decide the parameters of the MF.

In particular, the precision of the MPPT method depends on the increase in fuzzy rules while reducing the speed of the tracking ability. Few attempts have been made to balance both accuracies and tracking speed with the synchronization of FLC and traditional controllers. In view of the above, the combination of fuzzy and PID with a derivative filter (N)-based MPPT algorithm is proposed in this work to improve the accuracy and tracking speed of the algorithm. The FPIDN-based MPPT method has two structures such as FLC

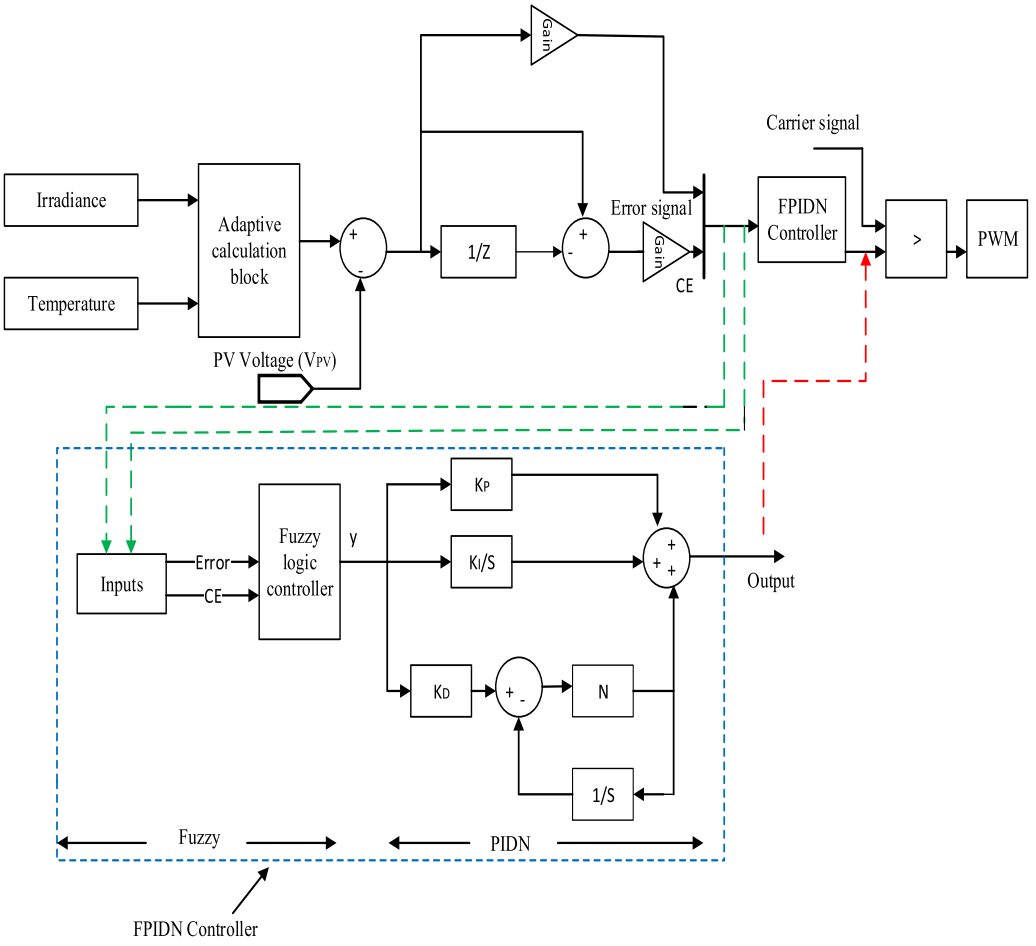

Fig. 4. The schematic arrangement of the adaptive FPIDN-based MPPT method.

and PIDN. The output of the FLC is y, which is carried out as input to the PIDN controller. The output of the PIDN is used to change the voltage for the dc-dc converter. The adaptive FPIDN-based MPPT method has been represented in Fig. 4.

The output of the PIDN can be expressed as:

$$\text{Output} = \left(y * K_P + \frac{K_I}{S} + \frac{S.N.K_D}{S+N}\right) \tag{7}$$

Where K_P is the gain of the proportional controller, K_I is the gain of integral, $K_D$is the derivative gain, and N is the derivative filter.

In this analysis, two blocks are considered in the MPPT method as the adaptive calculation block and FPIDN block. The adaptive calculation block produces a reference voltage for each MPP voltage($V_{MPP,ref}$). As the reference voltage is measured in the adaptive block, the rules of the fuzzy system can be reduced. The comparator compares the PV and reference voltages and the error signal ($V_{MPP,ref} - V_{PV}$) is assigned to the fuzzy as an input parameter. The crisp variables of the error signal are transmuted into the fuzzy parameters, which are recognized by the MF's in the fuzzy dataset and shown in Fig. 5(a)-(c). The fuzzy dataset consists of positive big (PB), positive small (PS), zero (ZE), negative big (NB), and negative small (NS).

The voltage and current values of the PV system under different weather conditions are mentioned as [18–20]:

The short circuit current (I_{sc}) is affected by the temperature and irradiance and indicated as:

$$I_{sc}^{*} = I_{sc}.\frac{G}{G_{STC}}\ (1 + X.\Delta T) \tag{8}$$

The open-circuit voltage is influenced by temperature and irradiance and mentioned as:

$$V_{oc}^{*} = V_{oc}.(1 + K.X.\Delta T).\ln\ (e + Z.\Delta G) \tag{9}$$

The consequence of current and temperature at MPP (I_{mpp})

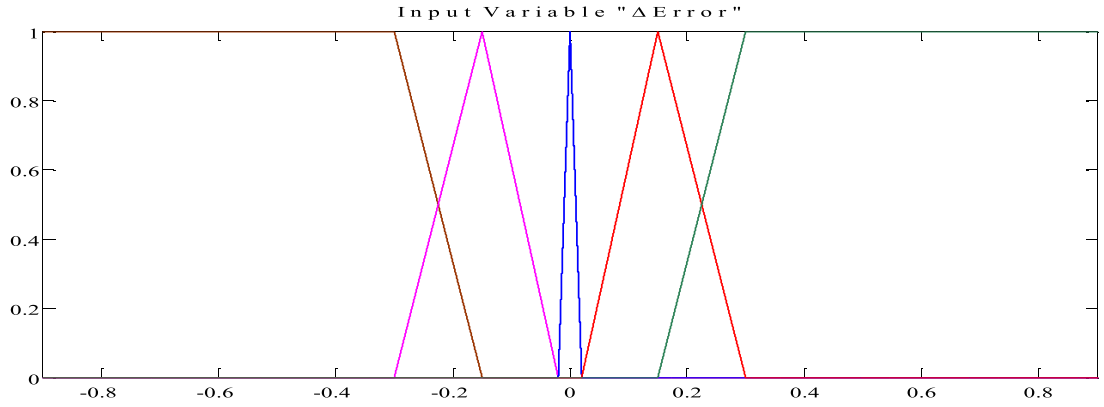

(a) change in error (CE)

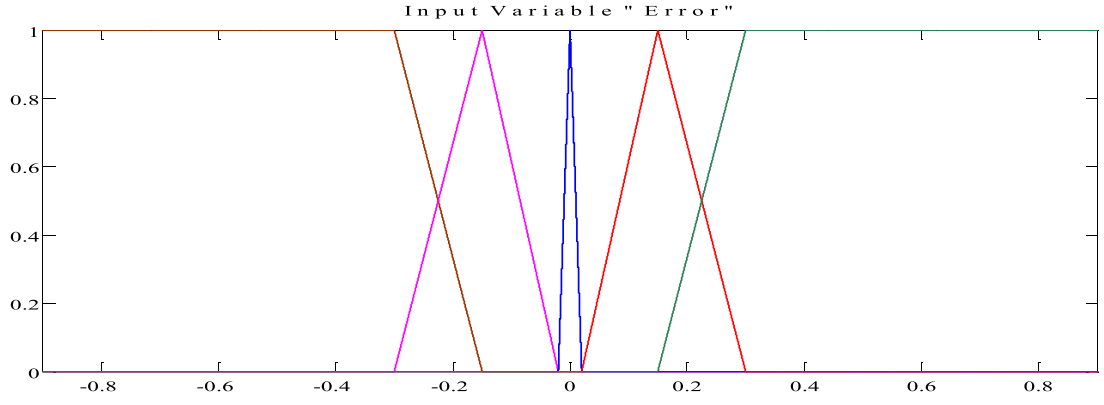

(b) Error

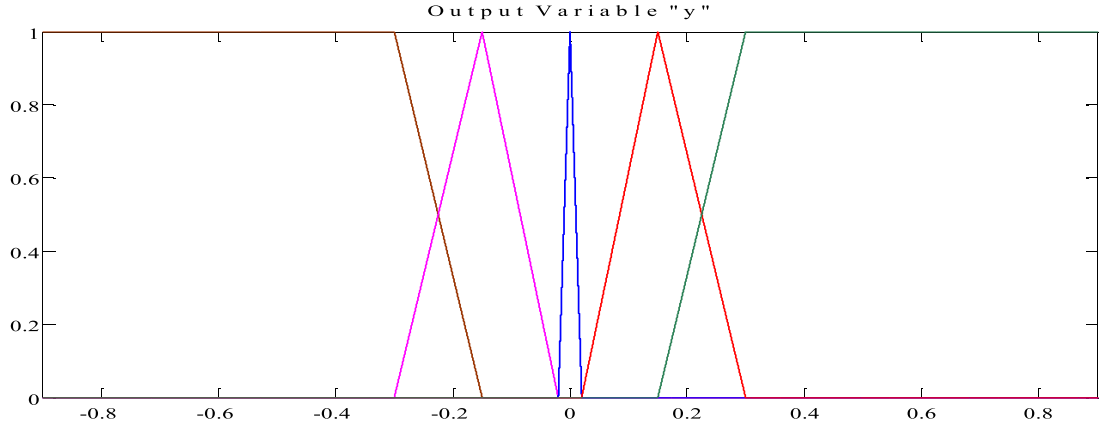

(c) Output (y)

Fig. 5. Membership functions.

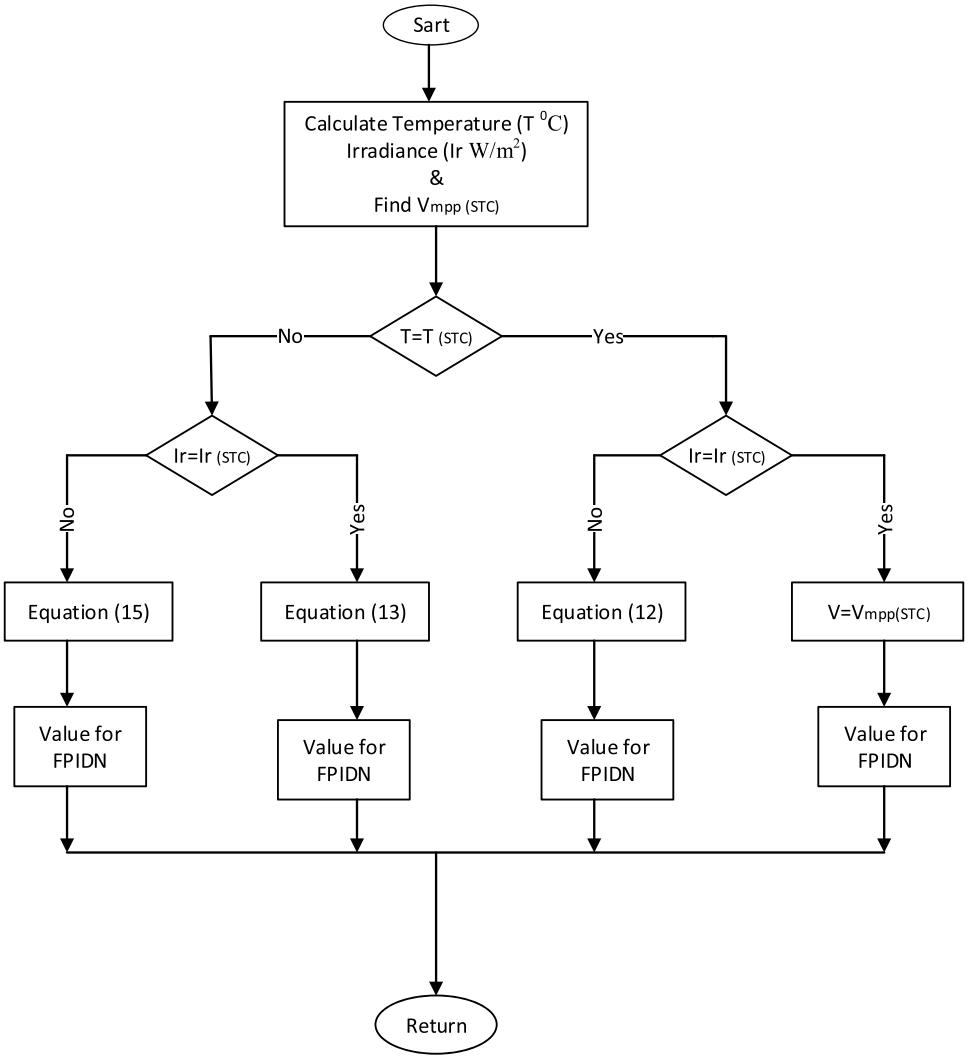

Fig. 6. The flowchart of reference voltage.

$$I_{mpp}{}^{*} = I_{mpp}\left(\frac{G}{G_{STC}}\right)(1 + X.\Delta T) \tag{10}$$

The consequence of voltage and temperature at MPP (V_{mpp})

$$V_{mpp}{}^{*} = V_{mpp}(1 + K.X.\Delta T).\ln(e + Z.\Delta G) \tag{11}$$

The reference voltage can be calculated from the Eq. (12)–(15).

If $\Delta G \neq 0$, $\Delta T = 0$, then (11) becomes:

$$V_{mpp}{}^{*} = V_{mpp}.\ln(e + Z.\Delta G) \tag{12}$$

In case, $\Delta G = 0$, $\Delta T \neq 0$ then (11) becomes:

$$V_{mpp}{}^{*} = V_{mpp}(1 + K.X.(T - T_{STC})) \tag{13}$$

From (12),

$$V_{mpp}{}^{*} = V_{mpp}.(1 + D.\Delta G) \tag{14}$$

If both cases are not equal to zero ($\Delta G \neq 0$, $\Delta T \neq 0$),

Table 2
System simulation parameters.

Symbol	Parameter	Numerical value
V_{mpp}	Rated Voltage	24.48 V
I_{mpp}	Rated Current	7.52 A
P_{mpp}	Rated Power	184 W
I_{sc}	Short-Circuit Current	8.15 A
V_{oc}	Open-Circuit Voltage	29.87 V
K_I	Temperature coefficient of I_{sc}	0.029 A/K
K_V	Temperature coefficient of V_{oc}	−0.33 V/K
N_{cell}	Number of cell modules	48
N_{se}	Number of series modules	11
N_{pa}	Number of parallel modules	09
L_{boost}	Inductor	5 mH
C_{boost}	Capacitor	250 μF
C_1	Input value of boost capacitor	100 μF
R_{Load}	Load Resistance	10 Ω
f_s	Switching Frequency	20 kHz
V_{in}	Boost converter input voltage	250 V–275 V
V_{out}	Boost converter output voltage	410 V–540 V
T_{sim}	Simulation Time	1 μs

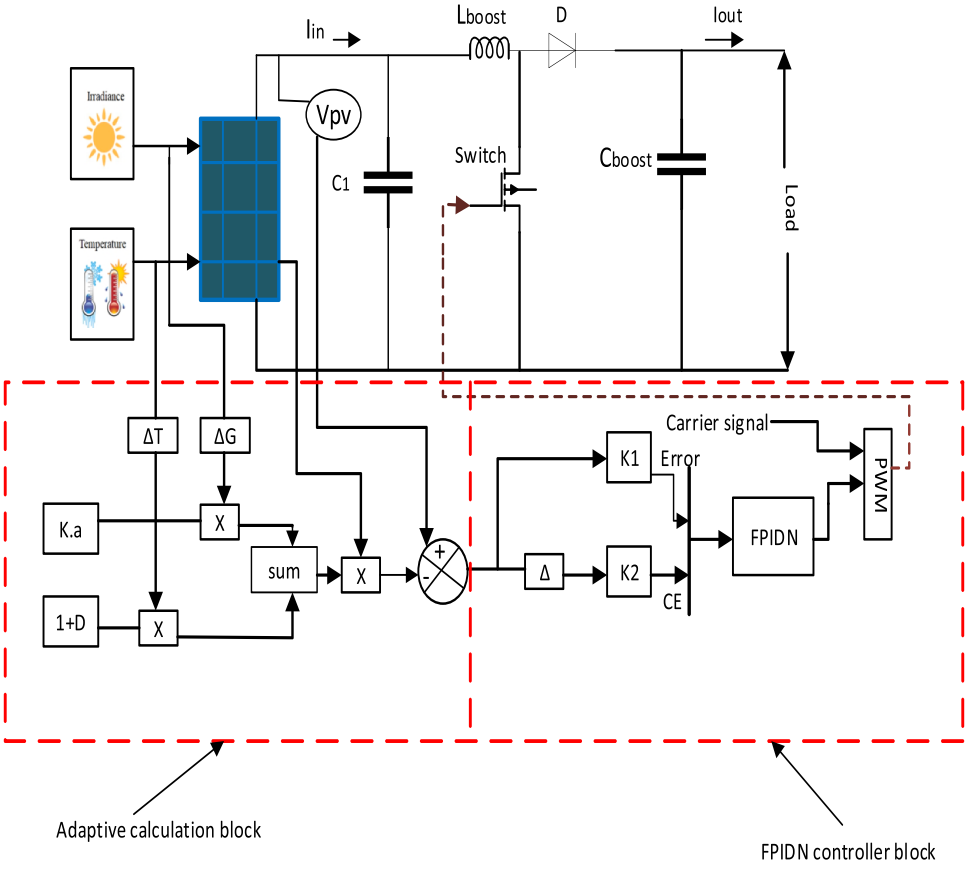

Fig. 7. The proposed system.

$$V_{mpp}{}^{*} = V_{mpp}(1 + K.X.(T - T_{STC})) + V_{mpp}.(1 + D.\Delta G) \quad (15)$$

In light of the above equations, K is the temperature coefficient (K=-0.32398), the voltage at MPP is V_{mpp}, X demonstrates the thermal coefficient (X=0.172, K*X=-38 mV/°C), G_{STC} is the irradiance at standard condition (1000 W/m^2), G illustrates the irradiance (W/m^2), T indicates the temperature (°C), T_{STC} is the temperature at standard circumstances (25 °C), Z=0.005, and D shows the consequence of irradiance at V_{mpp} ($0 < D < 1$).

The flowchart in the adaptive calculation module for the FPIDN controller is represented in Fig. 6.

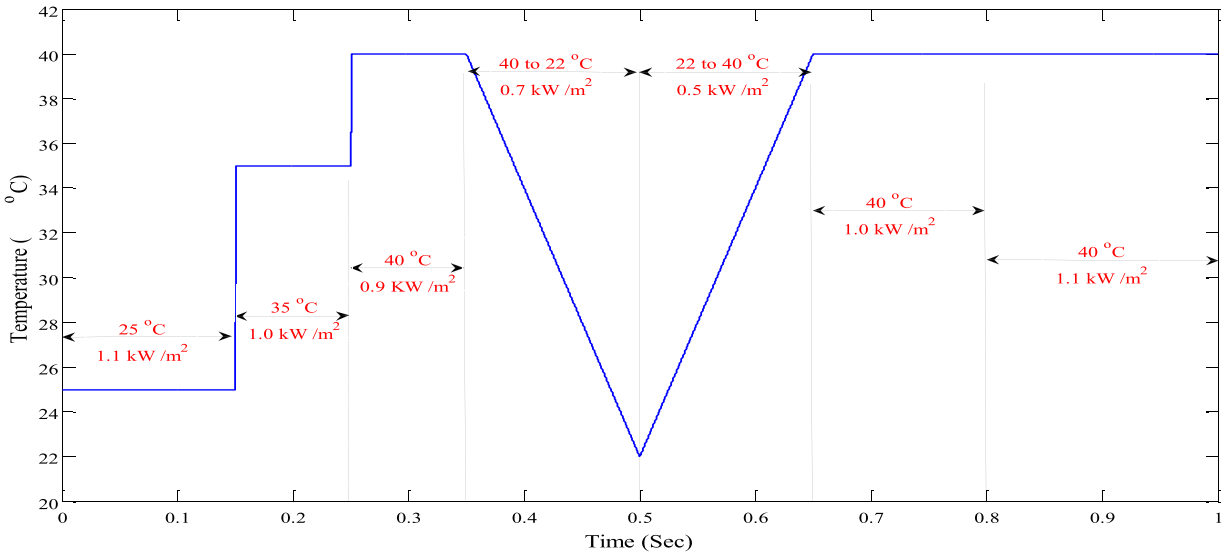

Fig. 8. Diverse temperature signals (°C).

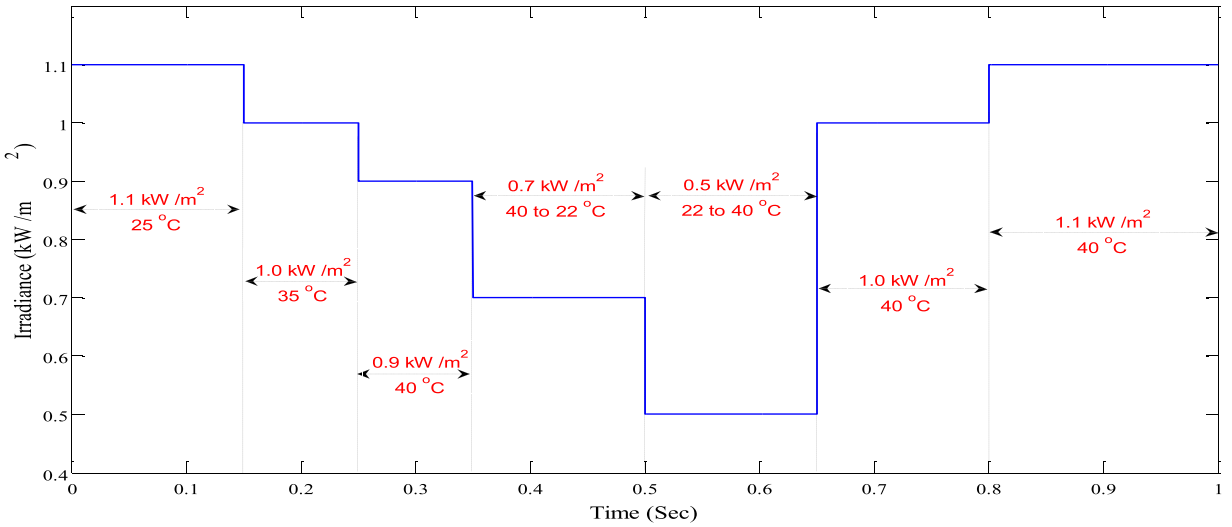

Fig. 9. Diverse irradiance signals (W/m2).

The method employs the following principle:

- If the value of irradiance is not identical to G_{STC} (1000 W/m^2) and the temperature is the same as T_{STC} (25 °C), then the V_{ref} is measured from the Eq. (12) and transferred to the FPIDN controller.
- If the value of temperature is not identical to T_{STC} (25 °C) and the irradiation value is the same as G_{STC} (1000 W/m^2), then the V_{ref} is evaluated from the Eq. (12) and the value is transferred to the FPIDN controller.
- If the values of irradiance and temperatures are not identical to G_{STC} (1000 W/m^2), T_{STC} (25 °C) respectively, then the V_{ref} is measured from the Eq. (15) and referred to the FPIDN controller.
- If the values of irradiance and temperatures are identical to G_{STC} (1000 W/m^2), T_{STC} (25 °C) respectively, then the V_{ref} is measured as $V_{mpp(STC)}$and transferred to the FPIDN method.

4. Results and discussions

This paper aims to provide a more detailed analysis on the characteristics of the PV system with a proposed MPPT method to various levels of irradiance and temperature. In this work, a new MPPT algorithm called the adaptive FPIDN method is used to regulate the duty cycle of the dc-dc converter and to generate the appropriate voltage. The proposed system is implemented in the MATLAB /

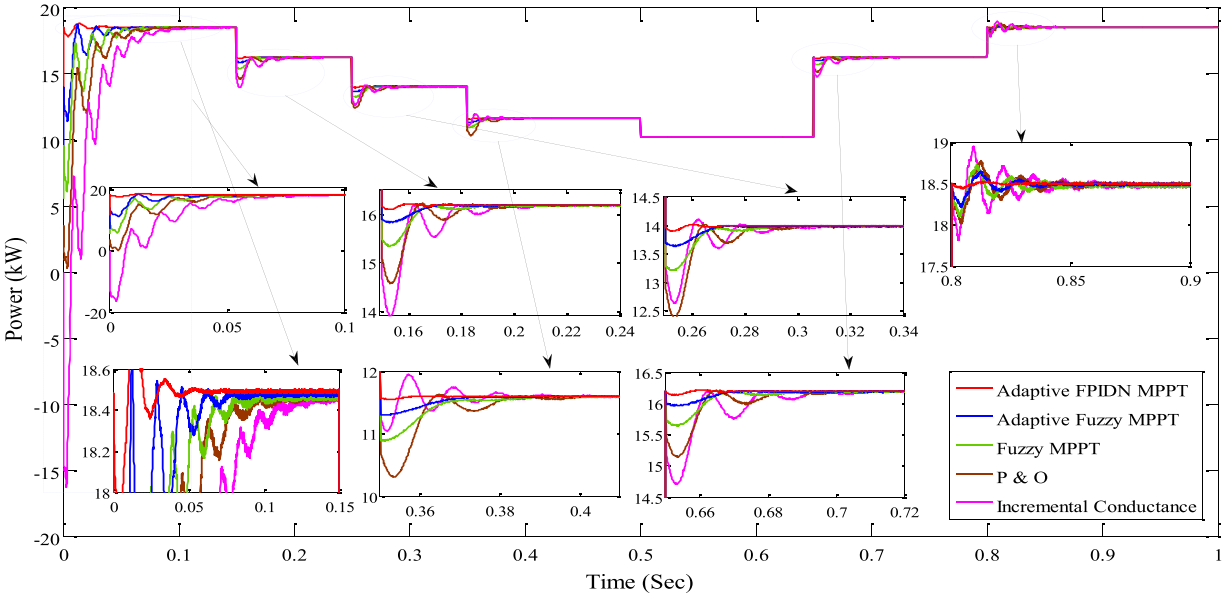

Fig. 10. The power of PV array with different MPPT methods.

Table 3
Comparative analysis of the five MPPT methods under all 7 states.

Parameter	States	Inc.Cond.	P &O	FLC	Adaptive FLC	Adaptive FPIDN
Voltage Ripple (V)	State 1	High	High	Less	Less	Negligible
	State 2	High	High	Less	Less	Negligible
	State 3	High	High	Less	Less	Negligible
	State 4	High	High	Less	Less	Negligible
	State 6	High	High	Less	Less	Negligible
	State 7	High	High	Less	Less	Negligible
Current Ripple (A)	State 1	High	High	Less	Less	Negligible
	State 2	High	High	Less	Less	Negligible
	State 3	High	High	Less	Less	Negligible
	State 4	High	High	Less	Less	Negligible
	State 6	High	High	Less	Less	Negligible
	State 7	High	High	Less	Less	Negligible
Settling time	State 1	0.15 s	0.09 s	0.062 s	0.057 s	0.048 s
	State 2	0.06 s	0.045 s	0.034 s	0.022 s	0.012 s
	State 3	0.059 s	0.041 s	0.031 s	0.015 s	0.008 s
	State 4	0.045 s	0.035 s	0.022 s	0.014 s	0.006 s
	State 6	0.038 s	0.029 s	0.018 s	0.012 s	0.004 s
	State 7	0.029 s	0.021 s	0.015 s	0.010 s	0.003 s
Convergence speed		0.15 s	0.09 s	0.062 s	0.057 s	0.048 s
Efficiency	State 1	96.72%	98.10%	98.92%	99.62%	99.72%
	State 2	95.32%	97.58%	98.65%	99.30%	99.51%
	State 3	96.45%	97.43%	98.82%	99.25%	99.62%
	State 4	96.98%	97.89%	98.64%	99.36%	99.65%
	State 6	96.43%	96.58%	99.01%	99.17%	99.49%
	State 7	95.03%	95.48%	98.74%	99.12%	99.45%

Simulink model. The simulation parameters [18,19] are shown in Table 2 and the suggested PV configuration is shown in Fig. 7.

In this work, the PV system was controlled using five distinct MPPT methods such as adaptive FPIDN, adaptive fuzzy, fuzzy, P&O, and Inc.Cond. Subsequently, the effectiveness of the proposed adaptive-based MPPT methods is ascertained through the comparative analysis of performance, speed, and accuracy under various temperature and irradiance conditions. Various temperature signals are demonstrated in Fig. 8, which range from 25 °C to 40 °C. Besides, the solar irradiance signals are represented in Fig. 9, range from 0.5 kW/m^2 to 1.1 kW/m^2. The changes in the temperature and solar irradiance of the system are classified into 7 states. State 1 shall be 1.1 kW/m^2 at 25 °C, State 2 is 1.0 kW/m^2 at 35 °C, State 3 is 0.9 kW/m^2 at 40 °C, State 4 is 0.7 kW/m^2 at 40 to 22 °C, State 5 is 0.5 kW/m^2 at 22 to 40 °C, State 6 is 1 kW/m^2 at 40 °C, and State 7 is 1.1 kW/m^2 at 40 °C.

The power output of the PV panel is determined with five different MPPT methods (adaptive FPIDN, adaptive fuzzy, fuzzy, P&O, and Inc.Cond.) under various irradiation and temperature levels, as shown in Fig. 10. The settling times for the studied MPPT methods

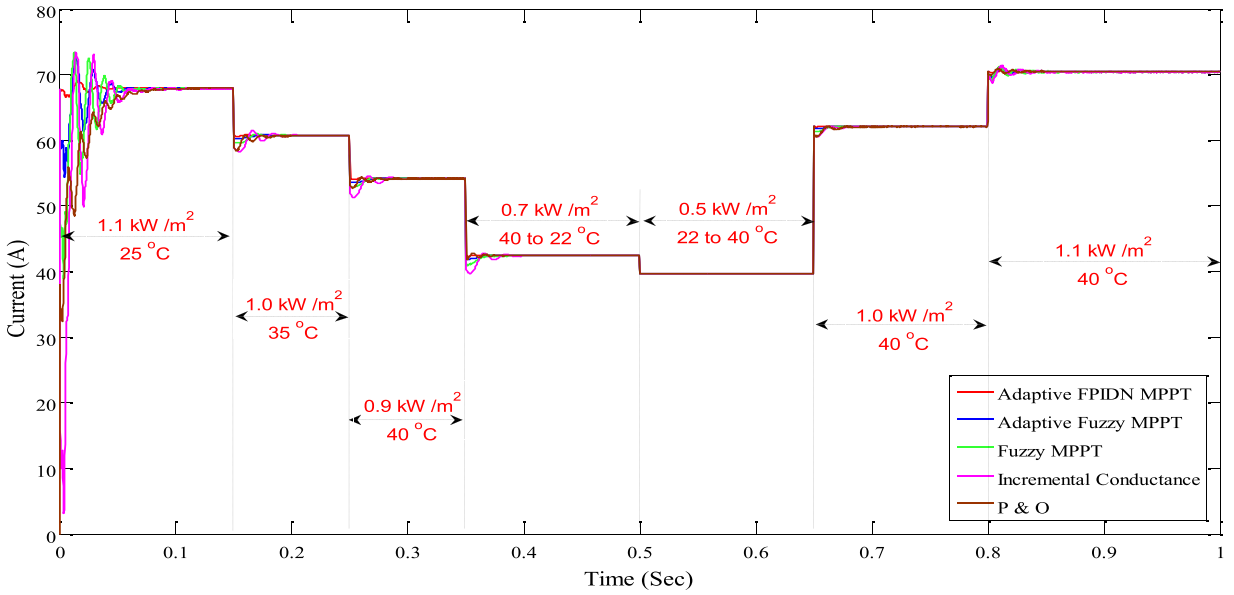

Fig. 11. The current of PV array with different MPPT methods.

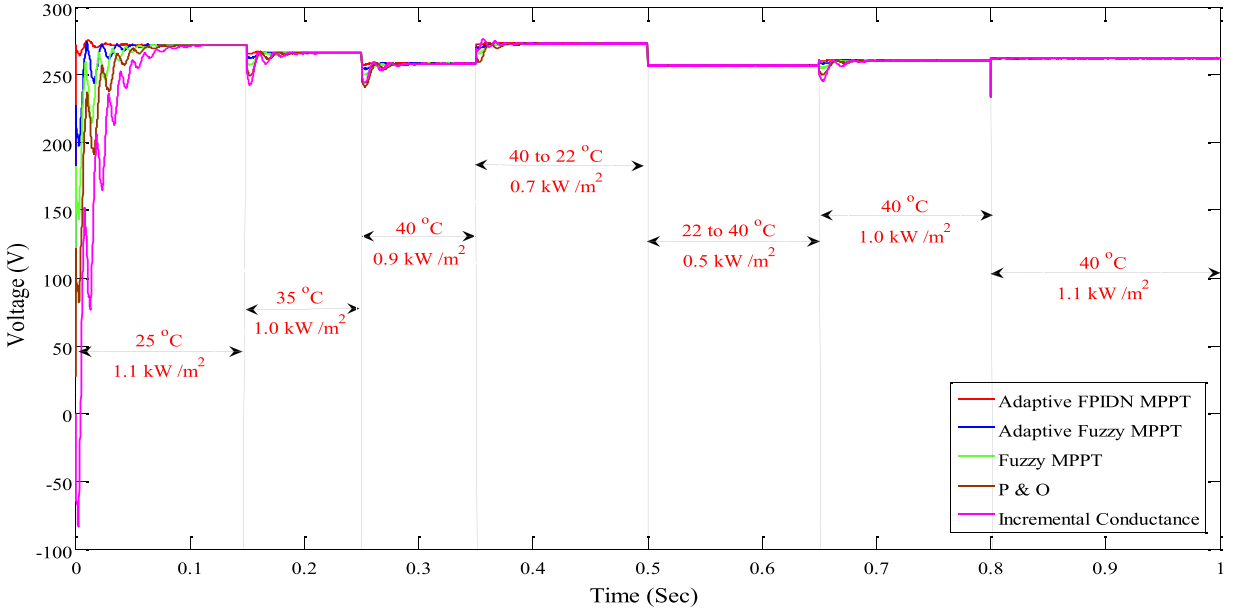

Fig. 12. The voltage of PV array with different MPPT methods.

have been found to be 0.048 s for adaptive FPIDN, 0.057 s for adaptive fuzzy, 0.062 s for fuzzy-based MPPT, 0.09 s for P&O, and 0.15 s for Inc.Cond. at all 7 states. However, the level of the irradiance is much lower in state 5, which not only eliminates current but also reduces the current fluctuations. It means that the loss of power is minimal. Therefore, state 5 has not been taken into consideration for analysis. The results of the numerical simulation show that the proposed adaptive FPIDN-based MPPT method provides the best output in all 7 states with different weather conditions. In addition, the speed of the proposed MPPT method is high compared to other studied methods for capturing the MPP. The numerical values for the efficiency of various MPPT methods are reported in Table 3.

Similarly, the current and voltage of the PV array are obtained using five different MPPT methods under various weather conditions are demonstrated in Figs. 11 and 12 respectively. Based on the simulation results, the proposed adaptive FPIDN-based MPPT method produces fewer oscillations in all 7 states. The performance analysis of the studied MPPT algorithms is shown in Table 3. The reference voltage of all 7 states generated using the adaptive FPIDN-based MPPT method under variable temperature and irradiance conditions are shown in Fig. 13.

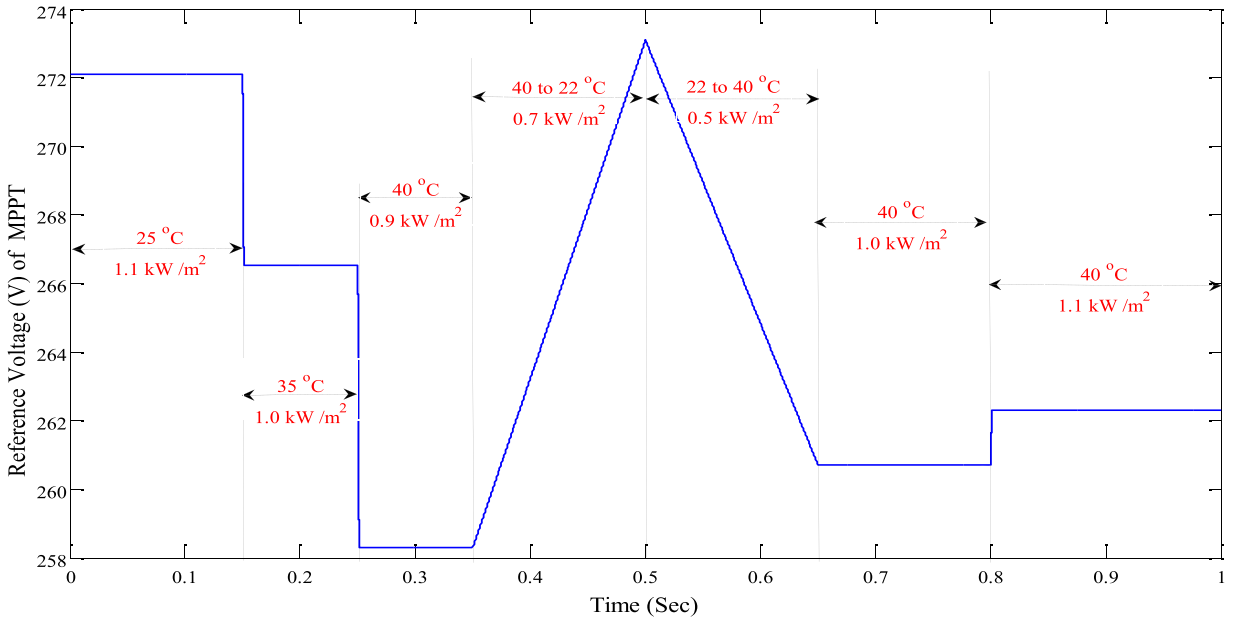

Fig. 13. Reference voltage of the MPPT algorithm.

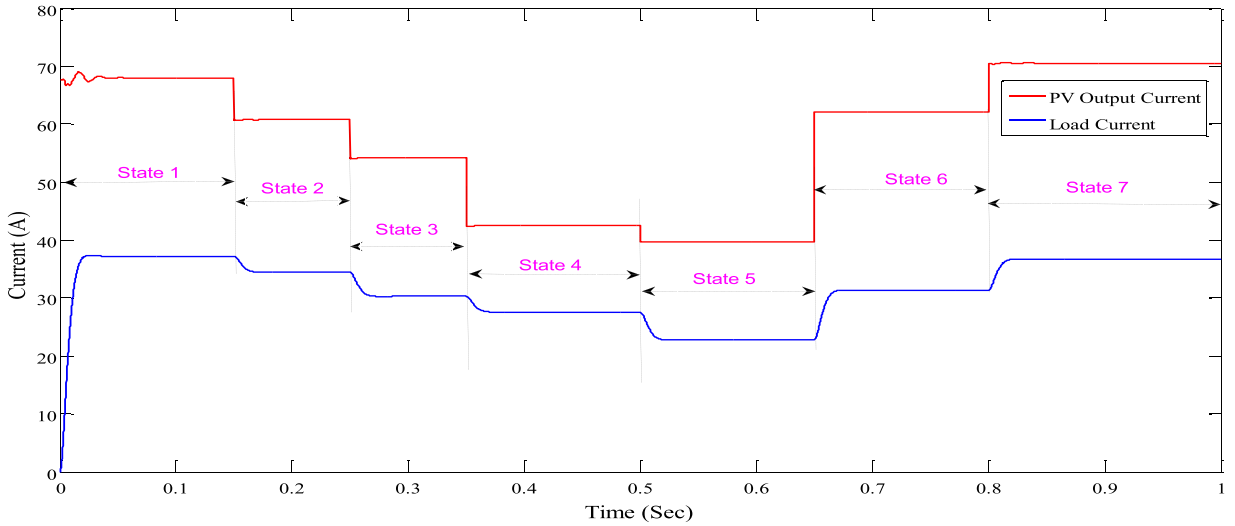

Fig. 14. Current values of PV array and boost converter.

The current and voltage output of the PV array and boost converter under variable atmospheric conditions are demonstrated in Figs. 14 and 15 respectively for all 7 states. Besides, the output power of the boost converter is shown in Fig. 16. The efficiency analysis of the MPPT methods studied ranged from 99.72 % to 99.45% for adaptive FPIDN, 99.62 % to 99.12 % for adaptive FLC, 98.92 % to 98.74 % for FLC based MPPT, 98.10 % to 95.48 % for P&O, 96.72 % to 95.03 % for Inc.Cond., and clearly presented in Table 3. It has been noted that the proposed adaptive FPIDN-based MPPT method has increased efficiency over other methods for all 7 states. Moreover, the efficiency and evaluation of the convergence time of the five MPPT methods are shown in Figs. 17 and 18 respectively. The proposed FPIDN-based MPPT has been assessed and compared with the other MPPT in Table 4.

5. Experimental validation

In order to determine the efficacy of the MPPT-based adaptive FPIDN technology, an experimental setup has been developed in the PV laboratory to validate the model results. The experimental setup of the system comprising of a PV panel, FPIDN controller, DSP controller (TMS320F28335), boost converter, and load is shown in Fig. 19. The booster converter is used for this work due to its

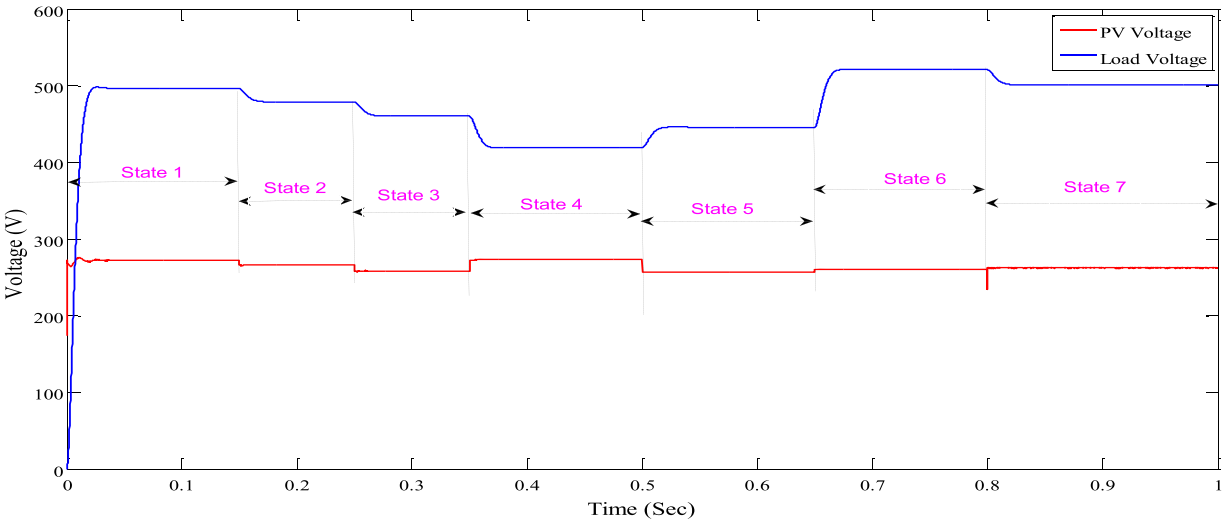

Fig. 15. Voltage values of the PV array and boost converter.

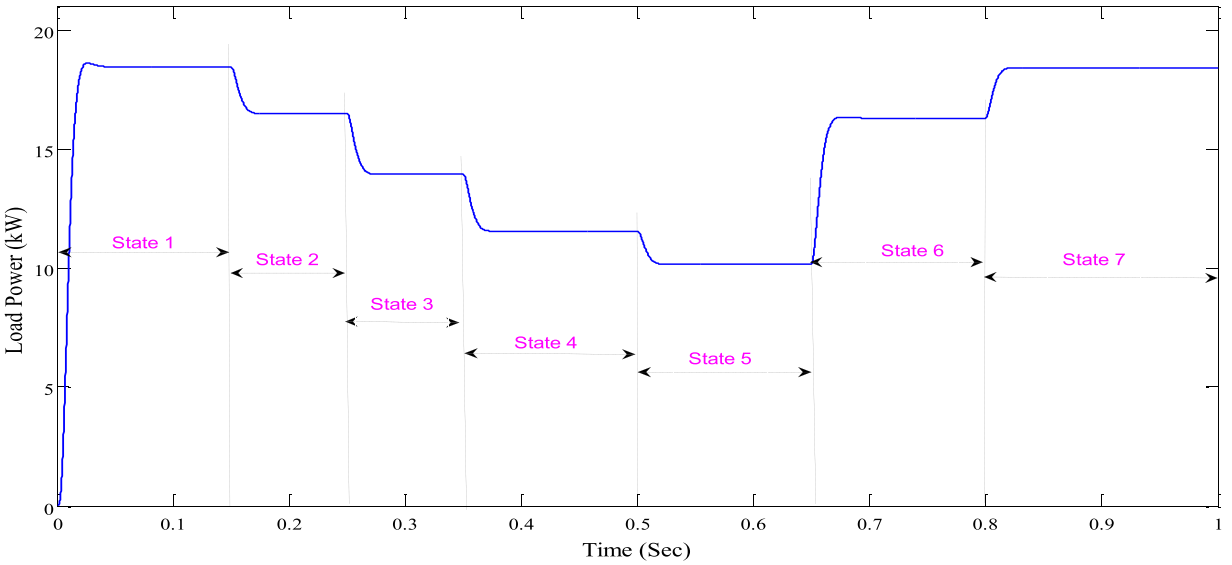

Fig. 16. Output power of boost converter.

reliability, ease of execution, and performance amongst other MPPT methods. The purpose of this boost converter is to bring the desired level of voltage from the PV output voltage. The boost converter has different components such as a switch (s), a capacitor (C), a diode (D), and an inductor (L). It operates on the principle of a dual control loop. The internal loop reduces the current flow in the inductor by regulating the service cycle, and the external loop regulates the voltage around the capacitor by altering the reference current. The inductor and capacitors are the main elements in the converter to boost the overall system performance [21]. Choosing an inductance value lower than the critical value, increases the system performance. Likewise, selecting the capacitance value smaller than the critical value, mitigates the ripples at converter resultant voltage. The critical values of the capacitor, inductor, and duty cycle of the switch are calculated-based on the following relations. [21]

$$D = \frac{V_{out} - V_{in}}{V_{out}} \tag{16}$$

$$C_{min} = \frac{D}{R\left(\frac{\Delta V_{out}}{V_{out}}\right) f_s} \tag{17}$$

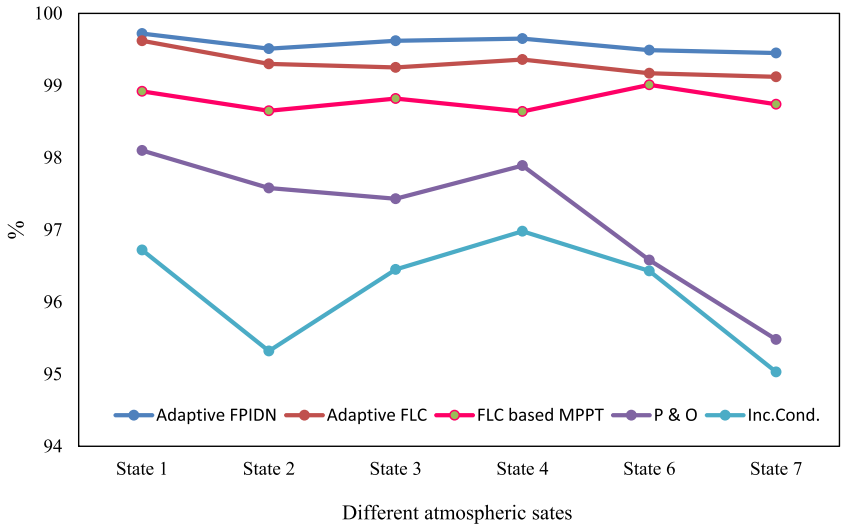

Fig. 17. Efficiency analysis of five MPPT methods.

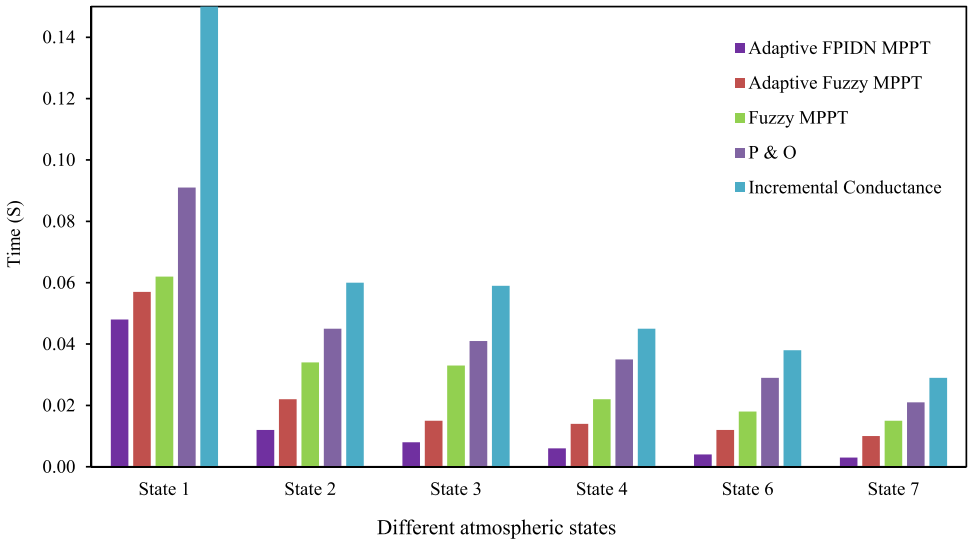

Fig. 18. Convergence time analysis of five MPPT methods.

Table 4
Comparison of suggested MPPT method with other existed methodses.

MPPT method	Efficiency	Capture time (s)	Economical Consideration	Fluctuations	Periodic Optimizing	System Inputs
P&O using FSCC [4]	97.56–95.71%	0.08	Moderate	Yes	No	Current, Voltage
Modified Inc.Cond. [8]	97.81–98.10%	0.069	Moderate	Yes	No	Current, Voltage
MFO based AI method [14]	98.25–99.91%	0.05464	Expensive	No	Yes	Voltage, temperature, irradiance
Fast converging method [7]	99.76–99.91%	0.051	Expensive	No	Yes	Voltage, temperature, irradiance
Suggested MPPT method	99.72–99.45%	0.048	Expensive	No	Yes	Voltage, temperature, irradiance

$$L_{min} = \frac{D(1-D)^2.R}{2f_s} \tag{18}$$

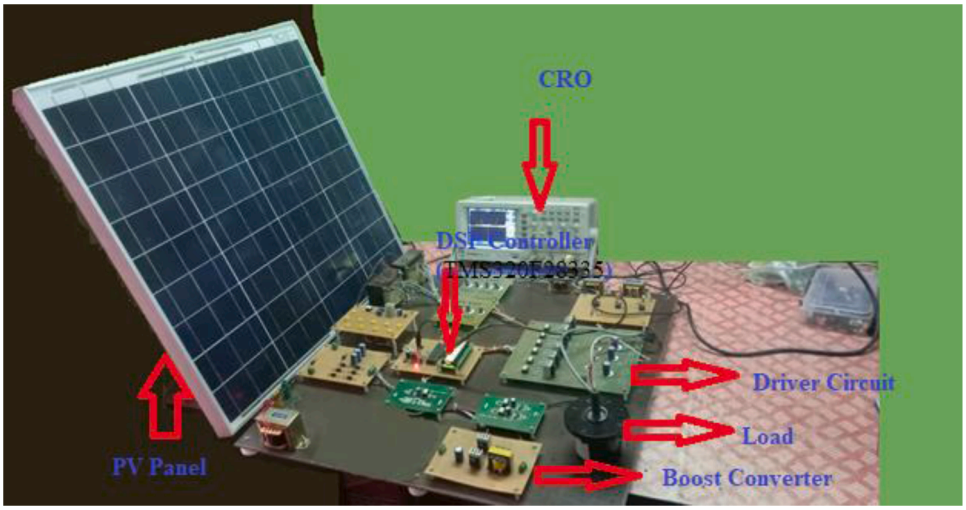

Fig. 19. Experimental setup of suggested PV system.

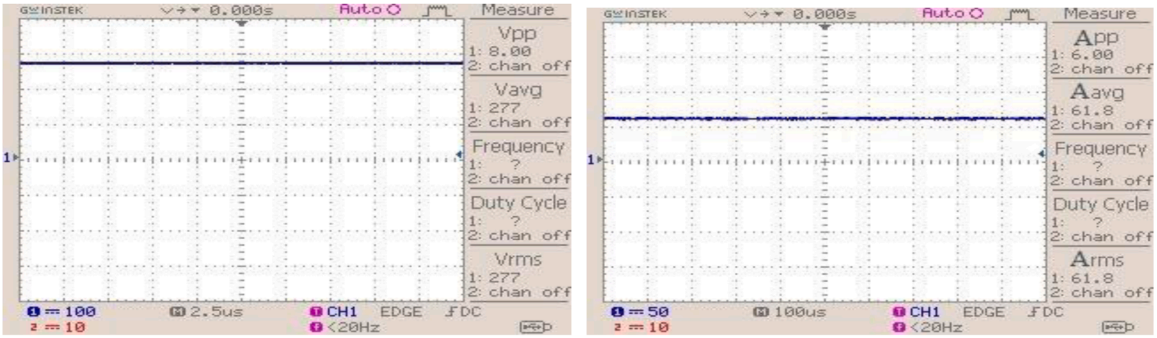

Fig. 20. The PV voltage and current at state 1 (1.1 kW/m^{2}at 25 °C).

Where D indicates the converter duty cycle; C_{min}, L_{min} represents the minimum values of the capacitor and inductor of the dc-dc converter respectively. f_s shows the switching frequency.

The current and voltage measurements from the PV panel at every operating stage is essential for performance validation. The measured open-circuit voltage (OCV) of PV is 29.87 V when it is not connected with the load through the suggested MPPT method. However, the new operating point of the PV panel with the proposed adaptive FPIDN-based MPPT depends on the load resistance. A new operating point can be reached to the MPP due to the significant changes in the duty cycle of the dc-dc converter using the adaptive FPIDN controller. Usually, several solar modules are interconnected to produce the maximum power output. In this analysis, 11 solar modules are connected in series to increase the output voltage, and 9 solar modules are presented in parallel to increase the resulting current. In most cases, solar cells are connected in series to increase the voltage. The PV voltage and current of state 1 (1.1 kW/m^{2}at 25 °C) is illustrated in Fig. 20 (a)-(b). Moreover, the load voltage, current, and power at state 1 are demonstrated in Fig. 21 (a)-(c).

Similarly, the PV voltage and current in state 2 (1.0 kW/m^2 at 35 °C) is shown in Fig. 22(a)-(b). It has been showed that the generated PV voltage is 275 V and the current is 59.5 A at state 2. In the presence of loading conditions, voltage, current, and power of the PV system are represented in Fig. 23(a)-(d). The load voltage, current, and power values are 481 V,36.1 A, 16.1 kW respectively. The experimental results are verified with the simulation responses of state 2 in Figs. 15 and 16. It should be noted that the results of the PV system are almost similar in both cases under state 2.

The irradiance value is decreased from 1.1 kW/m^2 to 0.9 kW/m^2 and the temperature has raised from 25 °C to 40 °C at state 3. The output of the PV panel for voltage and current is shown in Fig. 24(a)-(b). The voltage, current, and power under the load conditions, are demonstrated in Fig. 25(a)-(c). The experimental outcomes are compared with the simulation results and are presented in Figs. 15 & 16. It has been found that both the results are nearly close to each other at state 3.

The PV panel voltage and currents are 278 V & 57 A respectively at state 4. (Fig. 26(a)-(b)). Moreover, the PV system has been

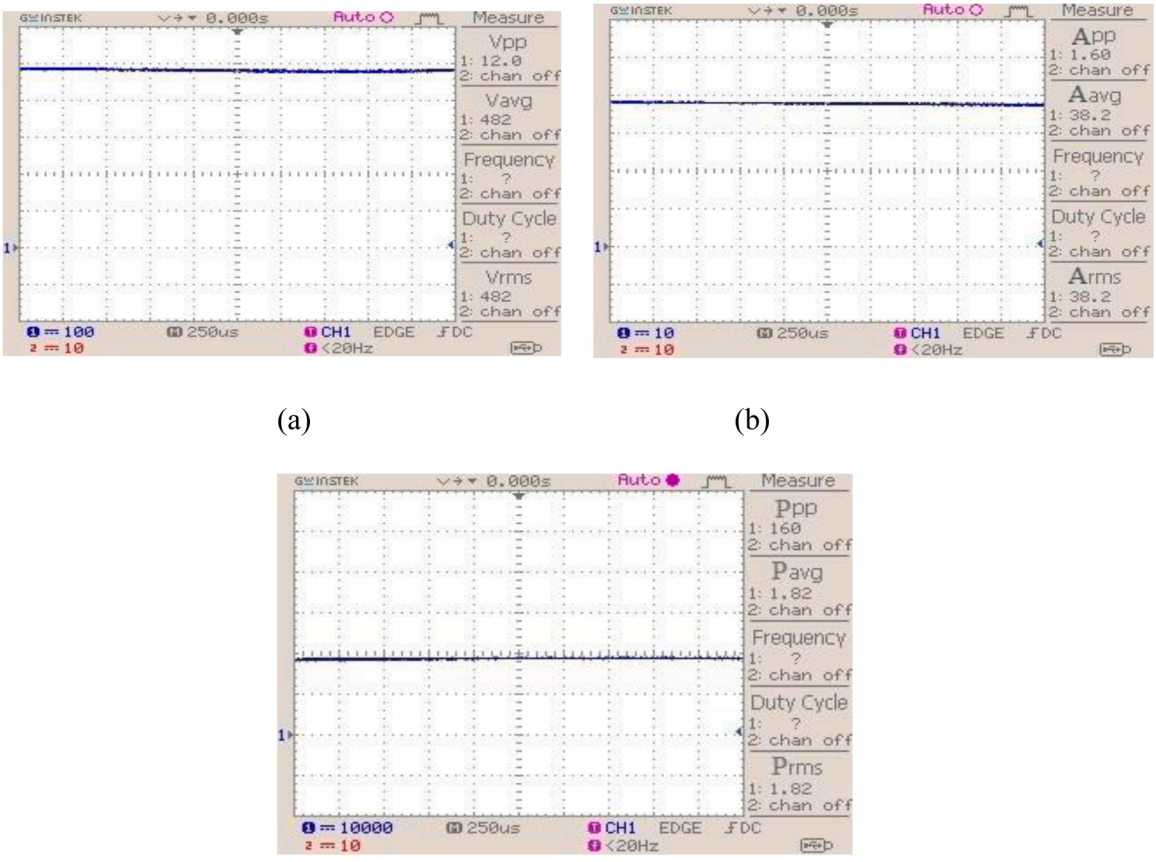

Fig. 21. The load voltage, current and power at state 1.

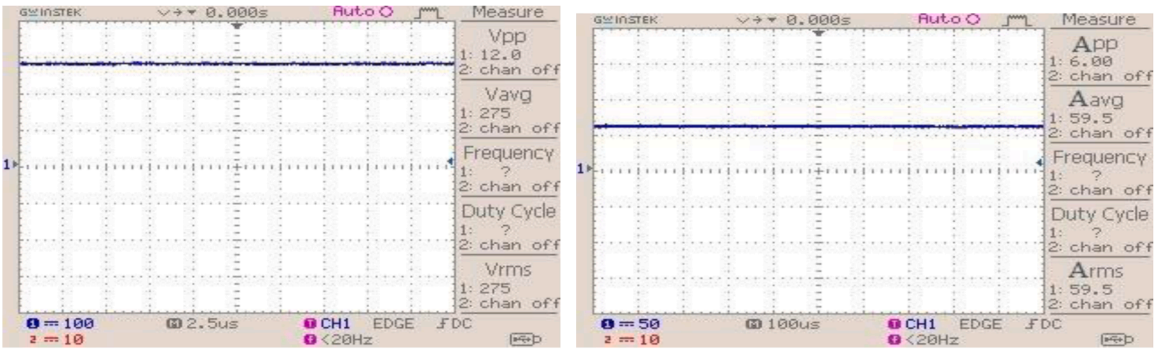

Fig. 22. Voltage and current of PV under state 2 (1.0 kW/m^2 at 35 °C).

tested with the load and observed voltage, current, and power are 462 V, 30.8 A,15.6 kW respectively. The performance of the boost converter at state 4 is compared with the simulation outcomes (Figs. 27(a)-(c), 5 &16). It should be noted that the performance results of state 4 are almost equal in both cases. Thus, it is proved that the suggested FPIDN-based MPPT method provided better performance under all states under varying atmospheric conditions.

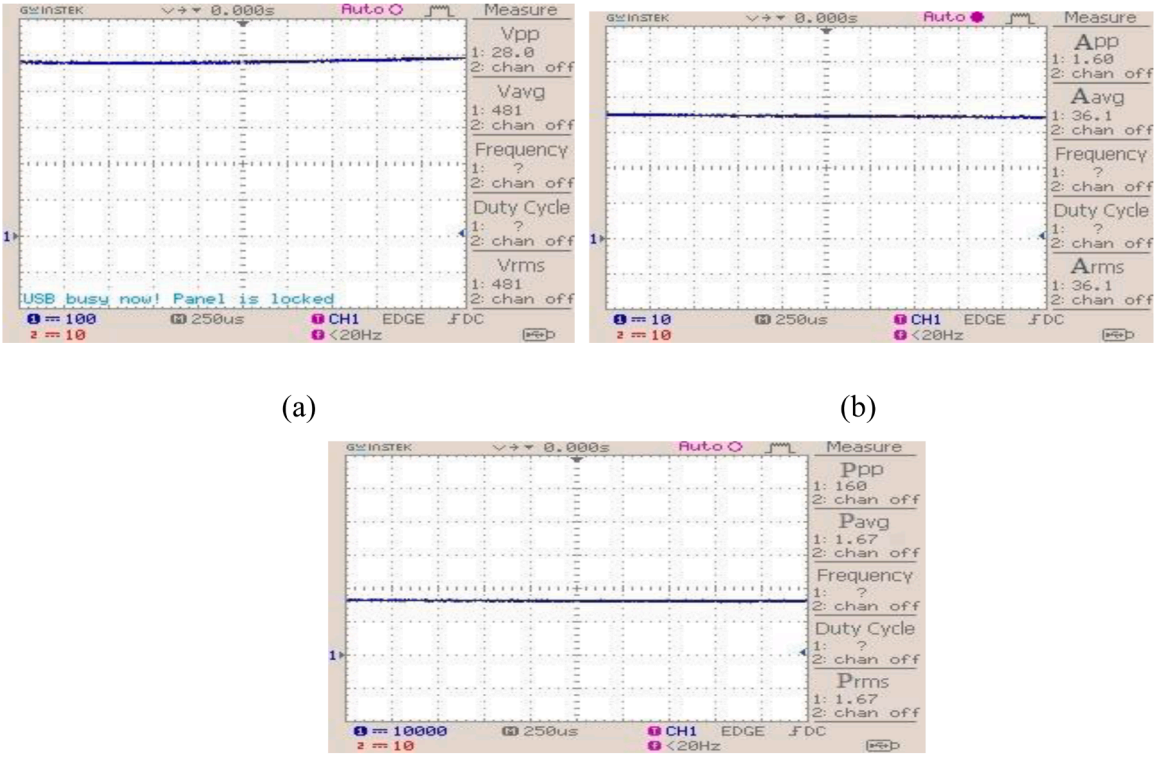

Fig. 23. Load voltage, current, and power at state 2.

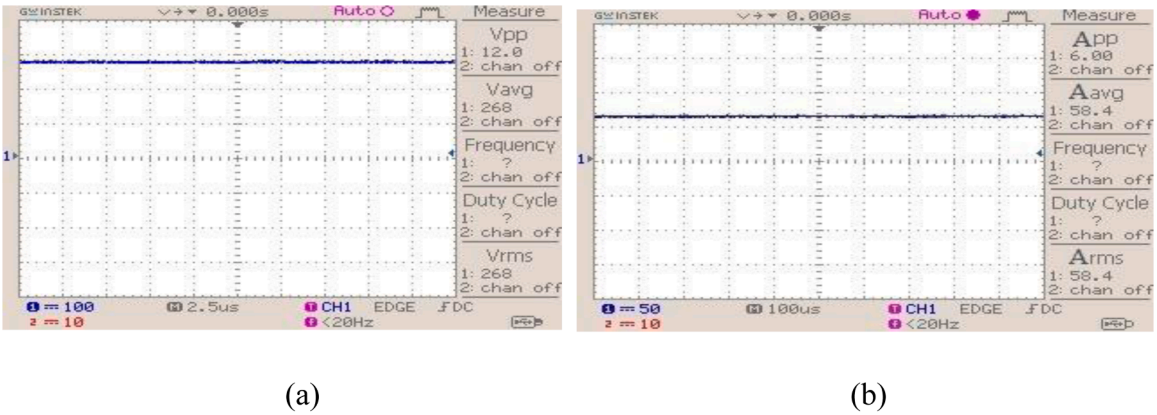

Fig. 24. The generation of PV voltage and current under state 3 (0.9 kW/m^2 at 40 °C).

6. Conclusion

This paper focuses on a new adaptive FPIDN-based MPPT algorithm for the PV systems, investigated under seven varying states of temperature and irradiance levels. The performance of the proposed method has been compared with various methods, namely adaptive FLC, FLC, P&O, and Inc.Cond. The results indicate that the proposed adaptive FPIDN-based MPPT method has shown a superior performance over other methods with respect to the rapid change in weather conditions. The settling times of the proposed adaptive FPIDN MPPT recorded at 0.048 s, outperforms of other methods with 15 % differences of the closest 0.057 s of adaptive fuzzy method, and 68 % of the worse 0.15 s for the Inc.Cond. method. Moreover, the efficiency of the proposed method recorded at 99.72 as compared to the closest performance recorded under adaptive FLC with 99.62 %, and 95.03 the worse of Inc.Cond. method. The results indicate that the proposed adaptive FPIDN-based MPPT method improves tracking speed, accuracy, and efficiency of the PV systems,

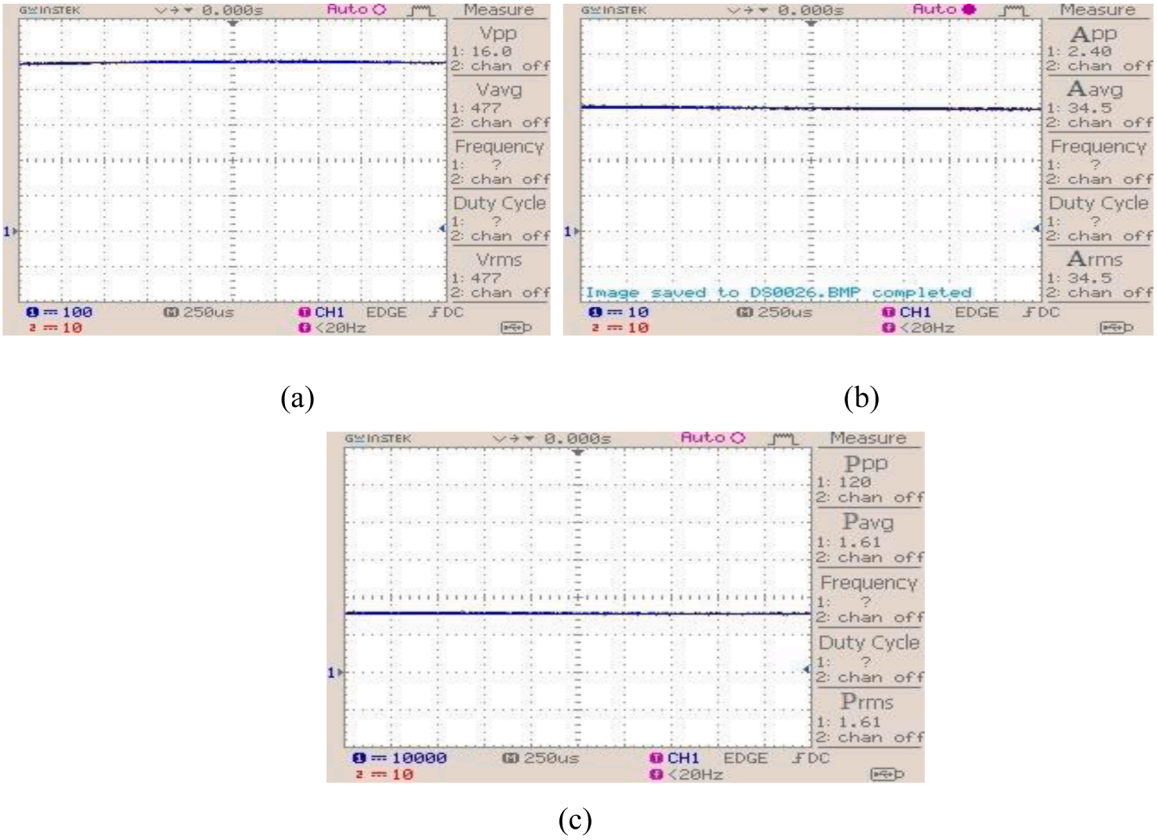

Fig. 25. Load voltage, current and power at state 3.

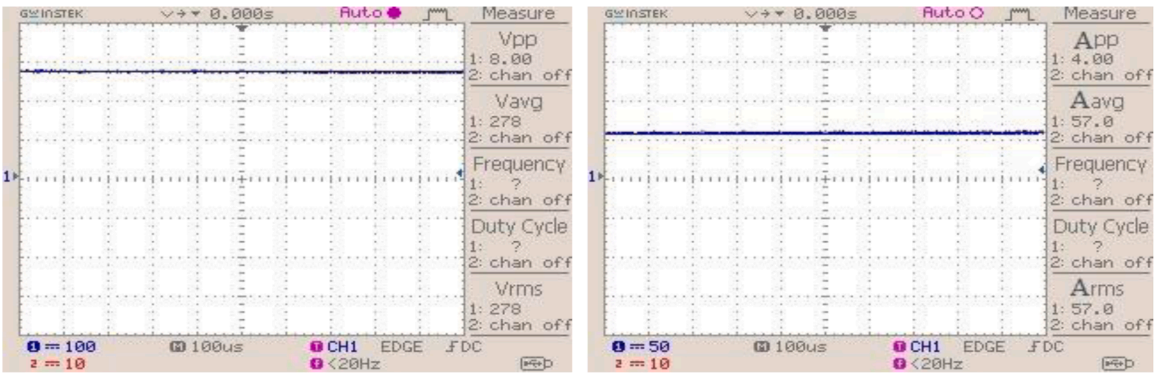

Fig. 26. The generation of PV voltage and current under state 4 (0.7 kW/m^2 at 22 °C).

under varying weather conditions.

Authorship statement

All persons who meet authorship criteria are listed as authors, and all authors certify that they have participated sufficiently in the work to take responsibility for the content, including participation in the concept, design, analysis, writing, or revision of the manuscript. Furthermore, each author certifies that this material or similar material has not been published elsewhere, accepted for publication elsewhere or under editorial review for publication elsewhere.

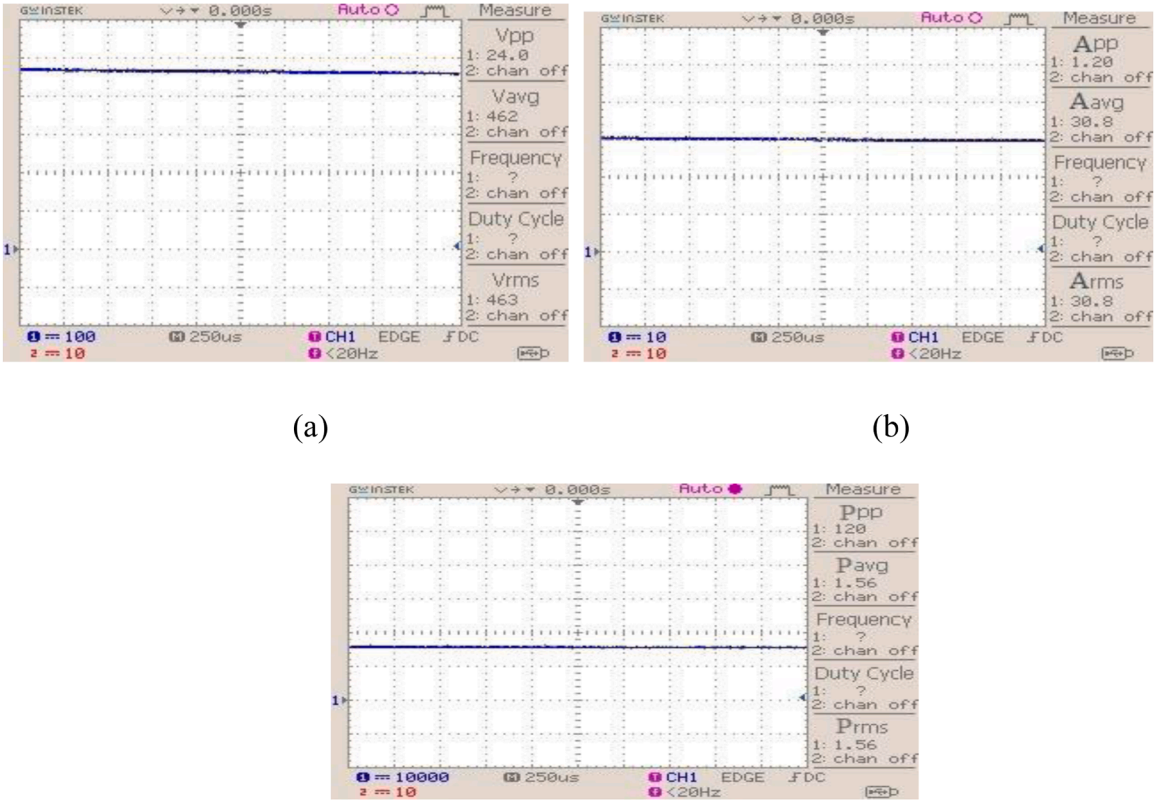

Fig. 27. Load voltage, current, and power at state 4.

Authorship contributions

P. Srinivasarao	Acquisition of data, drafting the manuscript, revising the manuscript, approval the version of manuscript to be published
K. Peddakapu	Acquisition of data, drafting the manuscript, analysis and/or interpretation of data, revising the manuscript, approval the version of manuscript to be published
M. R. Mohamed	Corresponding author, conception and design of study, analysis and/or interpretation of data, revising the manuscript critically for important intellectual content, approval the version of manuscript to be published
K.K. Deepika	Analysis and/or interpretation of data, revising the manuscript critically for important intellectual content, approval the version of manuscript to be published
K. Sudhakar	Drafting the manuscript, revising the manuscript, approval the version of manuscript to be published

Declaration of Competing Interest

The authors whose names are listed immediately below certify that they have NO affiliations with or involvement in any organization or entity with any financial interest (such as honoraria; educational grants; participation in speakers' bureaus; membership, employment, consultancies, stock ownership, or other equity interest; and expert testimony or patent-licensing arrangements), or non-financial interest (such as personal or professional relationships, affiliations, knowledge or beliefs) in the subject matter or materials discussed in this manuscript.

References

[1] Eltamaly AM, Farh HMH. Dynamic global maximum power point tracking of the PV systems under variant partial shading using hybrid GWO-FLC. Sol Energy 2019;177:306–16.
[2] Smadi IA, Rana A-Q. Explicit one-step model and adaptive maximum power point tracking algorithm for a photovoltaic module. Comput Electr Eng 2020;85:106659.
[3] Bendib B, Belmili H, Krim F. A survey of the most used MPPT methods: conventional and advanced algorithms applied for photovoltaic systems. Renew Sustain Energy Rev 2015;45:637–48.
[4] Sher HA, Murtaza AF, Noman A, Addoweesh KE, Al-Haddad K, Chiaberge M. A new sensorless hybrid MPPT algorithm based on fractional short-circuit current measurement and P&O MPPT. IEEE Trans Sustain Energy 2015;6(4):1426–34.

[5] Loukriz A, Haddadi M, Messalti S. Simulation and experimental design of a new advanced variable step size Incremental Conductance MPPT algorithm for PV systems. ISA Trans 2016;62:30–8.
[6] Soon TK, Mekhilef S. A fast-converging MPPT technique for photovoltaic system under fast-varying solar irradiation and load resistance. IEEE Trans Ind Informatics 2014;11(1):176–86.
[7] Li X, Wen H, Jiang L, Xiao W, Du Y, Zhao C. An improved MPPT method for PV system with fast-converging speed and zero oscillation. IEEE Trans Ind Appl 2016;52(6):5051–64.
[8] Farayola AM, Hasan AN, Ali A. Implementation of modified incremental conductance and fuzzy logic MPPT techniques using MCUK converter under various environmental conditions. Appl Sol Energy 2017;53(2):173–84.
[9] Reisi AR, Moradi MH, Jamasb S. Classification and comparison of maximum power point tracking techniques for photovoltaic system: A review. Renew Sustain Energy Rev 2013;19:433–43.
[10] Tey KS, Mekhilef S. Modified incremental conductance MPPT algorithm to mitigate inaccurate responses under fast-changing solar irradiation level. Sol Energy 2014;101:333–42.
[11] Hadji S, Gaubert JP, Krim F. Real-time genetic algorithms-based MPPT: study and comparison (theoretical an experimental) with conventional methods. Energies 2018;11(2):459.
[12] Kumar D, Chatterjee K. A review of conventional and advanced MPPT algorithms for wind energy systems. Renew Sustain Energy Rev 2016;55:957–70.
[13] Abido MA, Khalid MS, Worku MY. An efficient ANFIS-based PI controller for maximum power point tracking of PV systems. Arab J Sci Eng 2015;40(9):2641–51.
[14] Aouchiche N, Aitcheikh MS, Becherif M, Ebrahim MA. AI-based global MPPT for partial shaded grid connected PV plant via MFO approach. Sol Energy 2018;171:593–603.
[15] Safari A, Mekhilef S. Simulation and hardware implementation of incremental conductance MPPT with direct control method using cuk converter. IEEE Trans Ind Electron 2010;58(4):1154–61.
[16] Seyedmahmoudian M, Soon TK, Horan B, Ghandhari A, Mekhilef S, Stojcevski A. New ARMO-based MPPT technique to minimize tracking time and fluctuation at output of PV systems under rapidly changing shading conditions. IEEE Trans Ind Informatics 2019. https://doi.org/10.1109/TII.2019.2895066.
[17] Gowid S, Massoud A. A robust experimental-based artificial neural network approach for photovoltaic maximum power point identification considering electrical, thermal and meteorological impact. Alexandria Eng J 2020;59(5):3699–707. https://doi.org/10.1016/j.aej.2020.06.024.
[18] Yilmaz U, Turksoy O, Teke A. Improved MPPT method to increase accuracy and speed in photovoltaic systems under variable atmospheric conditions. Int J Electr Power Energy Syst 2019;113:634–51.
[19] Rezk H, Aly M, Al-Dhaifallah M, Shoyama M. Design and hardware implementation of new adaptive fuzzy logic-based MPPT control method for photovoltaic applications. IEEE Access 2019;7:106427–38.
[20] Rana KPS, Kumar V, Sehgal N, George S. A Novel dPdI feedback based control scheme using GWO tuned PID controller for efficient MPPT of PEM fuel cell. ISA Trans 2019;93:312–24.
[21] Huang YP, Hsu SY. A performance evaluation model of a high concentration photovoltaic module with a fractional open circuit voltage-based maximum power point tracking algorithm. Comput Electr Eng 2016;51:331–42.

P. Srinivasarao is a Lecturer at the Department of Electrical & Electronics Engineering, Nalanda Institute of Engineering and Technology, India. He received his B.Tech in Electrical Engineering from Prakasam Engineering College, Kandukur, M.E in Power System Automation from SRKR, Bhimavaram. His research interests are Renewable Energy, Power Electronics and optimization approaches.

K. Peddakapu received his B.Tech in Electrical Engineering from KIET, Kakindad, M.E in Power System Automation from SRKR, Bhimavaram and currently in final year of his PhD research at College of Engineering, Universiti Malaysia Pahang, Malaysia. His research interests are Renewable Energy, Power Systems Operations and Control and optimization approaches.

M.R. Mohamed is an Associate Professor at the College of Engineering, Universiti Malaysia Pahang. He was awarded his Ph.D. from Universiti Malaysia Pahang in 2013 and also hold M.Eng. in Electrical Engineering from UTHM, Malaysia, as well as B.Eng. in Electronic Engineering from University of Warwick, UK. His research interests are Renewable Energy, Energy Storage, Energy Harvesting, Power Systems, and Soft Computing.

K.K. Deepika received her B.Tech. in Electrical & Electronics Engineering from Nagarjuna University, M.Tech. in Electrical Engineering from GITAM University. She is pursuing her Ph.D. in Electrical Engineering at KLEF, India. She is working as a Lecturer in the Electrical & Electronics Engineering department of Vignan's Institute of Information Technology, India. Her research interests are Power Quality and Renewable Energy.

K. Sudhakar is a Senior Lecturer at the Faculty of Mechanical and Automotive Engineering Technology, Universiti Malaysia Pahang. He obtained his B.E in Mechanical Engineering from GCE, Salem, Madras University, and M.Tech in Energy Management from DAVV, Indore. He received his PhD from the NIT Trichy. He has been actively involved in teaching & research in the area of Renewable Energy.